NASA TECHNICAL MEMORANDUM

NASA TM X-3221

NASA TM X-3221

EFFECT OF WALL EDGE SUCTION ON THE PERFORMANCE OF A SHORT ANNULAR DUMP DIFFUSER WITH EXIT PASSAGE FLOW RESISTANCE

Albert J. Juhasz

Lewis Research Center

Cleveland, Ohio 44135

NATIONAL AERONAUTICS AND SPACE ADMINISTRATION • WASHINGTON, D. C. • APRIL 1975

1. Report No.	2. Government Accession No.	3. Recipient's Catalog No.
NASA TM X-3221		

4. Title and Subtitle	5. Report Date
EFFECT OF WALL EDGE SUCTION ON THE PERFORMANCE OF A SHORT ANNULAR DUMP DIFFUSER WITH EXIT PASSAGE FLOW RESISTANCE	April 1975
	6. Performing Organization Code
7. Author(s)	8. Performing Organization Report No.
Albert J. Juhasz	E-8149
	10. Work Unit No.
9. Performing Organization Name and Address	505-03
Lewis Research Center National Aeronautics and Space Administration Cleveland, Ohio 44135	11. Contract or Grant No.
	13. Type of Report and Period Covered
12. Sponsoring Agency Name and Address	Technical Memorandum
National Aeronautics and Space Administration Washington, D.C. 20546	14. Sponsoring Agency Code

15. Supplementary Notes

16. Abstract

The effect of wall edge suction on the performance of a short annular dump diffuser having a perforated plate flow resistance device in the exit passage was evaluated. Testing was conducted with air at near ambient pressure and temperature at inlet Mach numbers of 0.18 and 0.27 with suction rates up to 13.5 percent. Results show that pressure recovery downstream of the perforated plate was improved significantly by suction. Optimum performance was obtained with the flow resistance plate located at one inlet passage height downstream of the dump plane.

17. Key Words (Suggested by Author(s))	18. Distribution Statement
Combustor flow control Diffuser bleed	Unclassified - unlimited STAR category 34 (rev.)

19. Security Classif. (of this report)	20. Security Classif. (of this page)	21. No. of Pages	22. Price*
Unclassified	Unclassified	32	$3.75

* For sale by the National Technical Information Service, Springfield, Virginia 22151

EFFECT OF WALL EDGE SUCTION ON THE PERFORMANCE OF A SHORT ANNULAR DUMP DIFFUSER WITH EXIT PASSAGE FLOW RESISTANCE

by Albert J. Juhasz

Lewis Research Center

SUMMARY

The performance of a short annular dump diffuser equipped with the capability of applying suction (i.e., bleed) at both the inner and outer wall edges was evaluated with each of two perforated plates placed at three different positions downstream of the plane of abrupt area change. These plates, with a nominal solidity of 60 percent, were intended to simulate the effect of blockage presented by typical swirl can combustor arrays proposed for gas turbine engines.

The diffuser had an inlet flow area of 304 square centimeters (47.12 in.^{2}) followed by a dump approach section with an included divergence angle of 7°. The overall diffuser exit-to-inlet area ratio was 4.0. The (variable) diffuser length was determined by the location of the perforated plates which were successively positioned downstream of the plane of abrupt area change at distances equal to 0.5, 1.0, and 2.0 times inlet passage height. Velocity profile and diffuser pressure recovery measurements were taken downstream of the perforated plates at a distance of 0.5 times inlet passage height. These measurements were made at diffuser inlet Mach numbers of 0.18 and 0.27 with suction (bleed) rates ranging from zero to 13.5 percent of inlet mass flow rate. All testing was conducted with air at near ambient pressure and temperature.

Test results show that the jet flow type profiles obtained downstream of the plates without suction could be flattened considerably at 10 to 13.5 percent total suction by proper balancing of the suction flows such that about 42 percent of the total suction was applied at the inner wall and 58 percent on the outer wall. Hub biased profiles were obtained if more than 42 percent of the total suction was applied at the inner wall and tip biased profiles resulted if more than 58 percent of the total suction was applied at the outer wall.

The diffuser pressure recovery performance was also improved by suction as indicated by a maximum increase in diffuser effectiveness of about 70 percent and a reduction in total pressure loss by about one third.

INTRODUCTION

An investigation was conducted to determine the effect of wall suction on the exit velocity profile and pressure recovery of a short annular dump diffuser with exit passage flow resistance simulating the flow resistance of a modular, swirl can type, gas turbine combustor. The advantages of short diffuser-combustor systems in gas turbine applications, such as reduced engine length and weight, are discussed in reference 1. A drawback of short diffusers is that they usually incur severe performance losses, caused by flow separation. Reference 2 proposed and reported on the use of diffuser bleed (suction) to reduce performance losses and to control the exit velocity profile of a short annular diffuser with circular arc wall contours. A more simple design for a short diffuser is one having an abrupt area change between its inlet and exit flow passages. This device is usually referred to as a dump diffuser. This type of diffuser has been used in full-scale swirl can combustor tests as discussed, for example, in reference 3. However, no diffuser wall suction (i.e., bleed) was used during these tests and data on diffuser performance per se were not obtained. A simple dump diffuser consisting of a two-dimensional duct with a variable step area change on its lower wall followed by a suction slot was tested in reference 4. It is interesting to note that these tests were motivated by the pioneering work of Ringleb (ref. 5) concerning observations of mountain ridge vortex flows which lead to the formation of snow cornices.

Results of reference 4 showed that smooth expansion of the flow downstream of the step area change could be obtained when sufficient suction per unit wall span was applied. In reference 6 similar conclusions were reached from an investigation on the effect of suction on flow in a pipe with a sudden enlargement. The required suction flow was found to vary with the suction slot design. For the design yielding maximum pressure recovery the required suction flow was about 7 percent. The work of reference 6 was extended from a tubular to an annular geometry with an area ratio of 4.0 in reference 7. Inner and outer wall suction was applied at the downstream edges of the walls, that is, at the plane of sudden area change, through circumferentially continuous slots. The design of the suction slots was arrived at by extrapolating the results of reference 6. Test results showed that the diffuser exit velocity profile could be controlled from a hub biased profile to a tip biased one by varying the ratio of outer-to-inner wall suction rate. Although the diffuser effectiveness was also raised significantly by using suction, the maximum effectiveness was limited to approximately 52 percent, a level below that desirable for gas turbine combustor applications, where diffuser performance is further penalized by the combustor dome pressure loss.

Hence, in projecting the performance of gas turbine combustor diffusers from simple rig tests the effect of blockage presented by the combustor snout and dome must be taken into account. This blockage in the diffuser exit passage, although imposing a pressure loss penalty on diffuser performance, helps to distribute the flow and thus

improves the exit velocity profile. This so-called "filling effect" caused by diffuser exit blockage was first studied quantitatively by McClellan and Nichols using bell-shaped diffusers with screens in the exit passage (ref. 8). The authors showed that the filling effect was real and that high diffuser efficiencies could be obtained. Reference 9 documents an investigation directed at explaining the mechanics of the filling process for flow through bell-shaped diffusers with screens. With decreasing porosity (i.e., increasing solidity) the screens were found to behave more nearly like a solid wall with an axisymmetric jet impinging on it. The resulting axisymmetric stagnation flow pattern, with the highest static pressure along the flow axis, bent the streamlines sharply toward the wall thus preventing flow separation. A similar filling process is assumed to occur in swirl can combustors of the type tested in reference 3. In these combustors about 90 percent of the diffuser inlet flow passes through the swirl module array into the combustor primary zone. Hence the downstream airflow distribution and total pressure loss caused by a typical swirl module array can be approximated by the airflow distribution and pressure loss caused by a simple perforated plate when located in the diffuser exit passage. Of course the plate should have a solidity and distribution of blockage areas as close to that of the swirl module array as possible.

In an effort to simulate the flow through a typical swirl can combustor having an upstream dump diffuser with suction capability, the diffuser of reference 7 was retested in the present investigation with two different perforated plates successively mounted in the diffuser exit passage. Both plates had the same solidity of 60 percent but different hole sizes and hole spacings. The inlet passage of the diffuser with a flow area of 304 square centimeters (47.12 in.^{2}) was followed by a dump approach section with an included angle of 7°. The area ratio of the approach section was 1.15 and the overall diffuser area ratio was 4.0. Velocity profiles, diffuser effectiveness, and total pressure loss data were obtained with each of two perforated plates at three different positions downstream of the plane of abrupt area change. Tests were made at nominal inlet Mach numbers of 0.18 and 0.27 with suction rates ranging from zero to 13.5 percent of total inlet flow. All testing was conducted with air at near ambient temperature and pressure.

SYMBOLS

AR diffuser area ratio

B suction flow fraction of total flow rate

b wall suction fraction of total suction

d hole diameter

g_c dimensional constant

H diffuser inlet passage height

L length between plane of abrupt area change and blockage plate

M average Mach number at an axial station

MR mass flow ratio = $\frac{\text{mass flow computed from profiles}}{\text{mass flow computed from air orifice data}}$

m mass flow rate

P average pressure at an axial station

p local pressure at a radial position

q dynamic pressure

R gas constant for air

S suction rate, percent of total flow rate

T temperature

V average velocity at an axial station

v local velocity at a radial position

X downstream distance

γ specific heat ratio

ϵ diffuser efficiency (eq. (5)), that is, efficiency of diffuser and flow resistance combination

η diffuser effectiveness (eq. (3)), that is, effectiveness of diffuser and flow resistance combination

σ perforated plate solidity, percent

Subscripts:

i inner wall

m maximum

o outer wall

r local value at a given radial position

t total

0 stagnation condition

1 diffuser inlet station

2 diffuser exit station, downstream of flow resistance

APPARATUS AND INSTRUMENTATION

Flow System

The investigation was conducted in the test facility described in reference 2. A schematic of the facility flow system is shown in figure 1. Pressurized air at ambient temperature is supplied to the facility by a remotely located compressor station. This air feeds the three branches of the flow system.

The center branch (identified as "main air line") is the source of airflow through the test diffuser. The air flowing through this branch is metered by a square-edged orifice installed with flange taps according to ASME standards. The air is then throttled to near atmospheric pressure by a flow control valve before entering a mixing chamber from which it flows through the test diffuser. The air discharging from the diffuser is exhausted to the atmosphere through a noise absorbing duct.

The two other branches of the flow system supply the two air ejectors which produce the required vacuum for the inner and outer wall diffuser bleed flows. The ejectors are designed for a supply air pressure of 68 newtons per square centimeter (100 psia) and are capable of producing absolute pressures down to 2.38 newtons per square centimeter (7.0 in. Hg).

The inner and outer diffuser wall bleed flows are also metered by square-edged orifices. These orifices are also installed with flange taps according to ASME specifications in the suction flow lines that connect the inner and outer diffuser wall bleed chambers to their respective ejector vacuum sources.

Diffuser Test Apparatus

The apparatus used in this investigation was essentially that of reference 7 but for a few modifications. A cross section including pertinent dimensions is shown in figure 2. As in reference 7 the centerbody that forms the inner annular surface is cantilevered from support struts located 30 centimeters (12 in.) upstream of the diffuser inlet passage. This construction minimized the possibility of strut flow separation having an undesirable effect on the circumferential profile of inlet velocity.

Diffuser Walls and Exit Passage Blockage

The removable walls forming the dump approach passage were positioned in the test apparatus as shown in figure 2. The wall geometry and suction slot details are shown in figure 3. Also shown in this figure are the inlet and exit instrumentation stations and the

three test positions of the perforated blockage plates in the diffuser exit passage. To prevent flow separation, upstream of the suction slots, the annular dump approach passage was designed with a conservative value of included divergence angle of 7°, resulting in a dump approach passage area ratio of 1.15 at a length-to-inlet height ratio of 1.25. The overall diffuser area ratio was 4.0 with the overall diffuser length being variable, as defined by the three test positions of the perforated blockage plate. The suction slot geometry was designed for maximum pressure recovery at suction rates of 3 to 5 percent on each wall by extrapolating the results of reference 6. The inner and outer suction chambers were formed by the void spaces of the hollow toroidal wall geometry.

The geometric details of the two perforated blockage plates used in the test program are given in table I. Although both plates had the same solidity (60 percent), the hole diameters on plate A were twice those of plate B. Consequently the hole discharge coefficients differed significantly for the two plates. Tests were conducted with each of the two plates successively positioned in the diffuser exit passage downstream of the dump (plane of abrupt area change) at L/H distances of 0.5, 1.0, and 2.0.

Diffuser Instrumentation

The essential diffuser instrumentation is indicated in figures 2 and 3. Diffuser inlet total pressure was obtained from three five-point total pressure rakes equally spaced around the annular circumference. Inlet static pressure was measured using wall taps in the vicinity of the inlet rakes.

Diffuser exit total and static pressures were obtained by using three nine-point pitot static rakes that could be rotated in a circumferential direction and translated axially. For this investigation these rakes were positioned a distance equal to the inlet passage height downstream of the perforated plate location. All rake pressures were measured using three Scanivalves, each ducting pressures from a maximum of 48 ports to a flush mounted ±0.69-newton-per-square-centimeter (±1.0-psid) strain gage transducer. The valve dwell time at each port was 0.2 second, or over three times the interval required to reach steady state. Continuous calibration of the Scanivalve system was provided by ducting known pressures to several ports. Visual display of pressure profiles was made available by also connecting all inlet rakes and two exit rakes to common-well manometers. The manometer fluid was dibutyl phthalate (specific gravity, 1.04).

All other pressure data such as orifice line pressures for the main air line and the subatmospheric bleed-air lines were obtained by use of individual strain gage pressure transducers. The temperatures of the various flows were measured with copper constantan thermocouples.

All data were remotely recorded on magnetic tape for subsequent processing with a digital data reduction program. In addition any test parameter could be displayed in the

facility control room by means of a digital voltmeter.

PROCEDURE

Performance Calculations

Using the digital data reduction program mentioned previously, the overall diffuser performance was evaluated in terms of the radial profile of exit velocity, diffuser effectiveness, total pressure loss, and diffuser efficiency. The values of the latter three figures of merit were expressed in percentages.

Intermediate computations included average static and total pressures, local and average Mach numbers and local- to average-Mach number ratios; that is, the equivalent of the local- to average-velocity ratios. The average pressures and Mach numbers at the diffuser exit, P_2, P_{02}, and M_2, were computed by trapezoidal integration using area ratio weighed pressures at the various radial positions. At the diffuser inlet, straight arithmetic averages were computed. Local Mach numbers for each pitot tube were computed from the compressible flow relation

$$M_r = \sqrt{\frac{2}{\gamma - 1}\left[\left(\frac{p_0}{p}\right)^{(\gamma-1)/\gamma} - 1\right]} \tag{1}$$

where p_0 and p represent the measured local total and static pressures and γ represents the specific heat ratio, set equal to 1.4 for the near ambient conditions of this investigation.

Diffuser and bleed airflow rates were computed from the respective orifice pressures and temperatures. As a check on the arithmetically averaged inlet Mach number a mean effective inlet Mach number was also computed by iteration from inlet airflow rate, total pressure, temperature, and area data from the identity

$$M_1 = \frac{\dot{m}_1}{P_{01}A_1}\sqrt{\frac{RT_{01}}{\gamma g_c}}\left(1 + \frac{\gamma - 1}{2}M_1^2\right)^{(\gamma+1)/2(\gamma-1)} \tag{2}$$

As a check on data validity, a rearranged form of equation (2) was also used to compute the mass flow ratios MR_1 and MR_2 at the inlet and exit stations, respectively. The velocity ratios at each radial position, needed to generate velocity profiles, were obtained from the circumferential averages of the local- to average-Mach number ratios. A plotting routine was used to generate the velocity profiles by computer with output on microfilm.

Diffuser effectiveness was computed from the following relation:

$$\eta = \frac{P_2 - P_1}{(P_{01} - P_1)\left[1 - \left(\frac{1 - B}{AR}\right)^2\right]} \times 100 \tag{3}$$

Equation (3) is an approximation expressing the ratio of actual to ideal conversion of inlet dynamic pressure to exit static pressure for the case of compressible flows through a diffuser with wall bleed for $M_1 \leq 0.5$ and $AR \geq 2$. For the conditions of the present study the use of equation (3) introduced an approximation error of less than 0.5 percent. A derivation of equation (3) and its limitations is shown in reference 10.

The total pressure loss was defined as

$$\frac{\Delta P_0}{P_{01}} = \frac{P_{01} - P_{02}}{P_{01}} \times 100 \tag{4}$$

Diffuser efficiency was computed from the relation

$$\epsilon = \frac{\left(1 + \frac{\gamma - 1}{2} M_1^2\right)\left(\frac{P_{02}}{P_{01}}\right)^{(\gamma-1)/\gamma} - 1}{\frac{\gamma - 1}{2} M_1^2} \times 100 \tag{5}$$

Equation (5) was derived in reference 11 for the case where the diffuser exit velocity is negligible. This restriction can be removed from equation (5), as shown in reference 10 by making a minor change in the definition and subsequent derivation of the diffuser efficiency parameter. Hence equation (5), as used in this report, relates the total energy level available at the exit of a diffuser, to the upstream total energy level with the inlet static enthalpy being the reference.

Test Conditions

Typical diffuser inlet conditions were the following:

Total pressure, N/cm^2 abs (psia)	9.9 to 10.66 (14.4 to 15.5)
Static pressure, N/cm^2 abs (psia)	9.6 to 10.14 (13.9 to 14.7)
Temperature, K (^oF)	276 to 282 (36 to 47)
Mach number	0.178 to 0.269
Velocity, m/sec (ft/sec)	60 to 89 (196 to 293)
Reynolds number (based on inlet passage height)	2.13×10^5 to 3.25×10^5
Bleed rate, percent of total flow	0 to 13.5

Units

The U.S. Customary system of units was used for primary measurements and calculations. Conversion to SI units (Systeme International d'Unités) is done for reporting purposes only. In making the conversion, consideration is given to implied accuracy, which may result in rounding off the values expressed in SI units.

RESULTS AND DISCUSSION

The effect of wall edge suction on the performance of an annular dump diffuser with exit passage flow blockage was evaluated in terms of radial profiles of velocity, diffuser effectiveness, and total pressure loss. Tests were conducted at nominal inlet Mach numbers of 0.18 and 0.27 and suction rates ranging from zero to 13 percent with each of two perforated plates successively positioned downstream of the dump plane at L/H values of 0.5, 1.0, and 2.0. The perforated plate details are shown in table I. Although the solidity and thickness of the two plates was the same, the hole diameters and hole spacings of plate A were twice those of plate B. The resulting differences in hole discharge coefficients and downstream turbulent mixing phenomena are reflected in the performance results which will be discussed subsequently. A summary of diffuser performance data is given in table II.

Radial Profiles of Velocity

The inlet and exit velocity profiles shown in figures 4 and 5 were generated by plotting the ratio of local velocity at a radial position to the average velocity in a particular

plane (inlet or exit) as a function of increasing radial span position. The local velocity at a given radial span position was obtained by taking the arithmetic average of local velocities at three circumferential locations. Circumferential variations from these averaged profiles were about ±2 percent at the diffuser inlet and about ±30 percent at the diffuser exit plane. The profile measurement errors as indicated by the mass flow ratios MR_1 and MR_2 ranged from ±2 percent at the diffuser inlet station to ±8 percent at the exit station.

Because of the high degree of similarity between profiles obtained at comparable suction rates and inner-to-outer wall suction flow ratios, only a few typical profiles are shown. However some pertinent profile information such as exit profile peak position and exit profile peak values v_{m2}/V_2 and v_{m2}/V_1 are shown for each data point in table II. The first of these values expresses the ratio of maximum exit velocity to average exit velocity. The second value shows the ratio of maximum exit velocity to average inlet velocity and as such gives an indication of the velocity reduction for the highest velocity streamline. Hence this value is also shown in the figure captions for each of the profiles shown. Dividing the second by the first value gives the average velocity ratio V_2/V_1 which ranges from 0.20 to 0.26 as expected for the diffuser geometry and flow conditions tested. For profiles with suction on both walls the fraction of total suction, b_i and b_o, applied on the inner and the outer wall is also shown on each profile figure.

The inlet and exit radial profiles of velocity for perforated plate A (large holes) at the $L/H = 1.0$ position are shown in figure 4 for a nominal inlet Mach number of 0.18 with various combinations of inner and outer wall suction.

Figure 4(a) shows the inlet and exit velocity profiles obtained without the use of suction. The measuring station was at an $L/H = 2$ downstream of the dump plane, that is, at an $L/H = 1$ downstream of the plate. Also shown for comparison is the exit velocity profile obtained in reference 7 without a flow blockage device in the diffuser exit passage. This profile was determined at an $L/H = 0.75$ downstream of the dump plane. A comparison of the two profiles indicates that the blockage plate alters the original jet-type profile to one that is less peaked and fills a greater portion of the exit passage. The flat, slightly hub-biased inlet velocity profile was not affected by exit passage flow restriction and, as will be shown in succeeding figures, it was also unaffected by inlet Mach number, plate blockage, or suction rate.

The effect of inner wall suction is shown in figure 4(b). It is significant to note that despite the presence of the flow blockage plate, the exit velocity profile downstream of the blockage shows a pronounced hub bias with only 3.25 percent suction on the inner wall. To produce a similar degree of tip bias, approximately 4.9 percent suction was required on the outer wall as shown in figure 4(c). Use of about 6.7 percent suction on the outer wall increased the tip bias as shown in figure 4(d).

With suction applied on both the inner and the outer wall the exit velocity profiles tended towards symmetry about the midregion of the diffuser exit passage, provided that

the inner and outer wall suction rates were applied in the proper ratio. With 2.75 percent inner and 6.6 percent outer wall suction rate (i.e., with an inner to outer wall suction flow split of 29.5 percent to 70.5 percent), the exit velocity profile (fig. 4(e)) was not changed much from that of figure 4(d). This indicated that the inner wall suction rate had to be increased to obtain a symmetric profile. With 4.7 percent inner and 6.6 percent outer wall suction rate, figure 4(f), a considerably flattened and practically unbiased profile was obtained. This suggests that the suction flow split between the inner and outer wall should be 42 and 58 percent, respectively, if a symmetric exit velocity profile is desired. This flow split is approximately equal to the area split between the inner annulus of the exit passage, bounded by the inner wall and the passage centerline, and the outer annulus, bounded by the passage centerline and the outer wall.

It should also be noted that the exit profiles were stable with suction applied on both walls in the ratio required for symmetric exit profiles. This is a significant improvement over the oscillating profiles obtained during the open diffuser tests of reference 7.

Profiles are not shown for the inlet Mach number of 0.27 or a plate L/H position of 2.0 because the profiles were quite similar at comparable suction rates to those of figure 4. At the L/H = 0.5 position the flow spreading was inadequate and jet flow existed downstream of the plate for all wall suction combinations.

The velocity profiles obtained with perforated plate B (smaller holes) at the L/H = 2.0 position are shown in figure 5, with the inlet Mach numbers as indicated. With this plate the flow spreading effect for the L/H = 0.5 and 1.0 plate positions was small and hence no profiles are shown for these positions. Figure 5(a) shows the inlet and exit velocity profiles obtained for the case of no wall suction. The profile measurements were made at an L/H = 3 downstream of the dump plane thus maintaining the separation between the plate and the exit instrumentation at an L/H = 1. Also shown (dashed curve) is the exit velocity profile obtained in reference 7 without blockage in the diffuser exit passage. As mentioned previously, the profile measurements in reference 7 were made at an L/H = 0.75 downstream of the diffuser dump plane. Comparison of the inlet velocity profiles shown in figure 5 with those of figure 4 shows that the inlet velocity profile was not altered by downstream plate blockage.

Moreover the high degree of similarity between the solid and dashed exit velocity profiles (fig. 5(a)) indicates that the flow filling effect obtained with perforated plate B was small. In both cases a jet-type flow profile was observed. Figure 5(b) shows the hub biased exit velocity profile obtained with 4.15 percent suction on the inner wall. The tip biased profile resulting from an outer wall suction rate of about 4.25 percent is shown in figure 5(c). As with plate A, the exit velocity profiles with suction on both walls tended to be symmetric about the centerline of the diffuser exit passage provided the inner and outer wall suction rates are properly adjusted. Profile flattening also occurs if the wall suction rates are sufficient. Figure 5(d), for example, illustrates a flow condition for which the wall suction rates, although almost in the correct ratio for

a symmetric profile, are inadequate for a flat exit velocity profile. Figure 5(e), on the other hand, does show a symmetric and flattened exit velocity profile obtained with suction rates of 5.5 and 8.5 percent respectively on the inner and outer diffuser wall. As in figure 4(f) the symmetric exit profile was also stable. However, the degree of profile flatness is somewhat less than that shown in figure 4(f) obtained with plate A even though the total suction in figure 5(e) is greater than in figure 4(f). A logical conclusion is that plate B (small holes) presented less resistance to the flow than did plate A (large holes). Since the solidity was the same for both plates the variation in flow resistance can only be explained by the difference in hole sizes and hole spacing. The same conclusion is reached by comparing the profiles of figures 4(a) and 5(a), both obtained without suction.

In summary, the results depicted in figures 4 and 5 show that the airflow distribution in a diffuser exit passage, downstream of a flow resistance device, such as a perforated plate or a swirl can combustor module array can be controlled by application of diffuser wall suction upstream of the flow restriction. Also, solidity alone is not a sufficient indicator of flow resistance, that is, plate pressure loss. Besides solidity the hole size and spacing are also significant factors in estimating the flow resistance of a perforated plate. For the two plates tested the one with the coarser hole pattern (larger holes and wider spacing) produced the higher flow resistance. With quantitative data on the effect of hole pattern on plate $\Delta P_o/q$ not available, simulation of combustor flow resistance by simple perforated plates can only be approximated by matching the total pressure loss of the diffuser-plate combination to the total pressure loss of the combustor being simulated. Of course, this may be an iterative procedure requiring the testing of more than one perforated plate before sufficiently close pressure drop matching is obtained. The pressure drop matching obtained with the perforated plates tested here will be discussed in a later section.

Diffuser Effectiveness

Diffuser effectiveness as defined in equation (3) is a measure of the static pressure recovery downstream of the flow resistance. For a combustor this parameter permits computation of primary zone static pressure which must be maximized for good ignition and flame-holding performance.

Figure 6 shows several crossplots summarizing diffuser effectiveness results, shown in table II, as a function of plate position with suction rate as a parameter. The rapid rise in effectiveness as either plate is moved from the $L/H = 0.5$ to the $L/H = 1.0$ position is readily apparent. Moving the plate further downstream to the $L/H = 2$ position leads to only a small increase in diffuser effectiveness without suction or with 5 percent suction. A small decrease in diffuser effectiveness occurs at 10 percent suction. Therefore the $L/H = 1$ plate position is considered to represent an overall

optimum diffuser exit flow blockage location particularly for applications where the diffuser-combustor length must be minimized.

The higher effectiveness values obtained with plate B corroborate the conclusions drawn from the exit velocity profile results (figs. 4 and 5), namely that plate B offered a lower resistance to the flow than did plate A. The results shown in table II for perforated plate A at the $L/H = 1$ position show that the effectiveness parameter increased from about -11.4 percent without suction to about 48.9 percent at a total suction rate of about 11.5 percent. For perforated plate B the effectiveness parameter increased from about 5.6 percent without suction to 52.6 percent at a total suction rate of 13.24 percent.

Diffuser Total Pressure Loss

The decrease of diffuser total pressure loss with suction rate is shown in figure 7(a) for perforated plate A and in figure 7(b) for perforated plate B. The inlet Mach number was approximately 0.26 for the data points plotted. The lower pressure loss levels shown for perforated plate B with its finer hole pattern (smaller holes at closer spacing) may be explained by the smaller scale of turbulence existing downstream of the plate resulting in lower levels of turbulent energy dissipation. These lower pressure loss data for plate B are also in agreement with previously discussed velocity profile and effectiveness results. For both plates there is a significant decrease in total pressure loss level as the plate position downstream of the dump is changed from $L/H = 0.5$ to $L/H = 1$. This may be due to the establishment of a trapped vortex upstream of the plate which aids the flow spreading process. As predicted by the previously discussed effectiveness results, the additional reduction in pressure loss obtained by moving either plate further downstream is negligible.

The pressure loss value obtained without suction for plate B at the $L/H = 1$ position is in reasonable agreement with the cold flow pressure loss measured for the swirl can combustor of reference 3. Isothermal pressure loss values for other, that is, nonswirl can-type combustors quoted in the literature were in close agreement with the pressure loss values obtained with plate A. This implies that the total pressure loss caused by typical combustor dome blockages can be simulated by perforated plates such as used here. However, to simulate primary zone and inner and outer annulus flow splits of nonswirl can-type combustors, a more accurate replica of the combustor is required than can be provided by simple perforated plates.

Diffuser Efficiency

The isentropic diffuser efficiency, as defined by equation (5), is a measure of the degree of total flow energy conservation between the diffuser inlet and exit stations. The relation between diffuser efficiency, diffuser effectiveness and total pressure loss is discussed in detail in reference 10. Values of diffuser efficiency for the test readings of this study are given in table II. These values are seen to be within 5 percent of the diffuser effectiveness values for the readings tabulated, indicating reasonable agreement between two methods of flow energy accounting.

Pertinence of Results to Combustor Design

This investigation was conducted to determine the combined effects of wall edge suction and exit passage flow resistance on the performance of an annular high area ratio dump diffuser. The flow resistance devices, consisting of perforated plates, were intended to simulate the flow obstruction of a gas turbine combustor dome. The diffuser was tested with each of two plates in three separate positions downstream of the dump plane and the results were compared to those of reference 7 wherein the same diffuser geometry was tested without exit passage flow resistance.

A swirl can combustor-type flow obstruction was found to aid the flow spreading process in the diffuser exit passage. The optimum position for the combustor flow obstruction downstream of the dump plane was found to be equal to one diffuser inlet passage height in installations where the minimum suction rate is expected to exceed about 6 percent. Below this total suction level the best performance is obtained with the combustor dome at the $L/H = 2$ position.

Of particular importance in combustor design is the result that the velocity profile or airflow distribution downstream of a flow resistance device can be controlled by using suction on the diffuser walls. Qualitatively this result suggests that the air flow distribution in a combustor can be tailored as in a variable geometry combustor to suit the requirements of a particular engine operating condition by using diffuser wall suction. Quantitative measurements of the actual airflow distribution in the primary zone and the hub and tip annuli would have to be performed using a more detailed replica of the combustor dome in model testing.

The pressure loss of the diffuser-combustor system was found to decrease with increasing suction rate. At total suction rates above 10 percent the performance of the diffuser-combustor system, including the perforated plate pressure loss penalty, was found to equal or exceed the performance of the open diffuser tested in reference 7. It is conceivable that the performance levels of the dump diffuser-combustor system could be raised by improvements in suction slot design. Hence, the suction rates required

for control of the combustor airflow distribution may be compatible with the turbine cooling requirements of high performance gas turbine engines.

SUMMARY OF RESULTS

The performance of a short annular dump diffuser with variable position exit passage flow resistance was evaluated. The diffuser was equipped with suction capability through peripheral edge slots on both the inner and the outer wall. The flow resistance devices consisted of two simple perforated plates, both of 60 percent solidity but of differing hole diameters and hole spacings. Tests were conducted with each of the two plates successively positioned at three different locations (L/H = 0.5, 1.0, and 2.0) downstream of the plane of abrupt area change. The performance results (effectiveness, pressure loss, and downstream velocity profiles) of the diffuser and flow resistance combination were as follows:

1. The optimum plate position for achieving the highest performance levels by the use of suction was determined to be the L/H = 1 position.

2. A significant drop in performance occurred with either plate at the L/H = 0.5 position.

3. With either plate at the L/H = 2 location performance levels at suction rates above 6 percent were only slightly below those obtained for the optimum L/H = 1 position. Below 6 percent total suction rate performance was slightly higher at the L/H = 2 position than at the L/H = 1 position.

4. Performance was independent of inlet Mach number but increased with suction rate for all plate positions.

5. For perforated plate A (larger holes with coarser spacing) at the optimum (L/H = 1) position, the overall system effectiveness increased from -11 percent without suction to 49 percent at a total suction rate of 11.5 percent.

6. The corresponding system total pressure loss at a nominal inlet Mach number of 0.26 was reduced from 5.1 percent at no suction to 3.1 percent at a total suction rate of 8.6 percent.

7. Performance levels were somewhat higher with perforated plate B (smaller holes with finer spacing) suggesting that the finer scale of turbulence occurring downstream of the plate resulted in a lower level of turbulent energy dissipation.

8. The velocity profiles downstream of the perforated plates could be made hub biased by applying more than 42 percent of the total suction on the inner wall and tip biased by applying more than 58 percent of the total suction on the outer wall of the diffuser.

9. Considerably flattened, symmetric and stable downstream velocity profiles were obtained at total suction rates of 10 percent or more, distributed between the inner and outer walls in the ratio of 0.42 to 0.58.

10. In simulating the airflow distribution and isothermal pressure loss of a swirl can combustor by a simple perforated plate, hole size, and spacing must be taken into account in addition to plate solidity.

11. Although the isothermal pressure loss of a non swirl-can-type combustor can be simulated by a perforated plate of the proper geometry, to simulate primary zone and annulus flow splits a detailed model of the combustor should be used.

Lewis Research Center,
National Aeronautics and Space Administration,
Cleveland, Ohio, December 17, 1974,
505-03.

REFERENCES

1. Roudebush, William H.: State of the Art in Short Combustors. ICAS Paper 68-22, Sept. 1968.

2. Juhasz, Albert J.; and Holdeman, James D.: Preliminary Investigation of Diffuser Wall Bleed to Control Combustor Inlet Airflow Distribution. NASA TN D-6435, 1971.

3. Niedzwicki, Richard W.; Juhasz, Albert J.; and Anderson, David N.: Performance of a Swirl-Can Primary Combustor to Outlet Temperatures of 3600° F (2256 K). NASA TM X-52902, 1970.

4. Heskestad, Gunnar: Remarks on Snow Cornice Theory and Related Experiments with Sink Flows. J. Basic Eng., ASME Trans., vol. 88, no. 6, June 1966, pp. 539-549.

5. Ringleb, F. O.: Flow Control by Generation of Standing Vortices and the Cusp Effect. Aero. Eng. Rept. 317, Princeton University, 1955.

6. Heskestad, Gunnar: Further Experiments with Suction at a Sudden Enlargement in a Pipe. ASME Paper 69-WA/FE-27, Nov. 1969.

7. Juhasz, Albert J.: Performance of a Short Annular Dump Diffuser using Wall Trailing-Edge Suction. NASA TM X-3093, 1974.

8. McLellan, Charles H.; and Nichols, Mark R.: An Investigation of Diffuser-Resistance Combinations in Duct Systems. NACA ARR L-329, 1942.

9. Schubauer, G. B.; and Spangenberg, W. G.: Effect of Screens in Wide-Angle Diffusers. NACA TN 1610, 1948.

10. Juhasz, Albert J.: Performance of an Asymmetric Short Annular Diffuser with a Nondiverging Inner Wall Using Suction. NASA TN D-7575, 1974.

11. Shapiro, Ascher H.: The Dynamics and Thermodynamics of Compressible Fluid Flow. Vol. 1, Ronald Press Co., 1953, pp. 151-152.

TABLE I. - PERFORATED PLATE DIMENSIONS

Perforated plate	Percent solidity, σ	Hole diameter, d, cm (in.)	Plate thickness, cm (in.)	Hole pattern
A	60	0.633 (0.25)	0.32 (0.125)	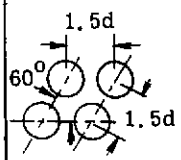
B	60	0.32 (0.125)	0.32 (0.125)	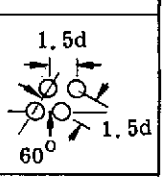

TABLE II. - DIFFUSER PERFORMANCE DATA

Reading	Diffuser inlet Mach number	Airflow rate		Inlet pressure				Inlet total temperature		Suction rate, percent			Exit profile (peak)			Diffuser effectiveness, percent	Diffuser efficiency, percent	Total pressure loss, $\Delta P/P$, percent
		kg/sec	lb/sec	Total		Static		K	°F	Inner wall	Outer wall	Total	Position, percent of annular span	Value, v_{m2}/V_2	Value, v_{m2}/V_1			
				N/cm^2	psia	N/cm^2	psia											
Perforated plate A at 2.5 cm (1 in.); L/H = 1.0																		
529	0.261	3.33	7.34	10.44	15.14	9.92	14.38	278	41	0	0	0	60	2.02	0.45	-11.2	-10.4	5.1
530	.261	3.33	7.34	10.45	15.15	9.92	14.39				0	0	60	2.02	.44	-11.7	-11.1	5.1
531	.260	3.32	7.33	10.37	15.04	9.85	14.28				2.36	2.36	40	1.78	.40	7.07	6.43	4.4
532	.263	3.33	7.34	10.37	15.04	9.85	14.28				2.37	2.37		1.76	.40	6.88	6.65	4.4
533	.264	3.33	7.34	10.34	15.00	9.82	14.24				3.43	3.43		1.83	.42	13.33	12.97	4.2
534	.265	3.34	7.37	10.34	15.00	9.82	14.25				3.41	3.41		1.83	.42	12.52	13.50	4.1
535	.265	3.34	7.36	10.33	14.98	9.81	14.23				3.96	3.96		1.80	.41	15.88	16.69	4.0
537	.264	3.33	7.34	10.32	14.97	9.81	14.22				4.37	4.37		1.86	.43	17.30	17.59	3.9
538	.263	3.32	7.32	10.32	14.97	9.81	14.22				4.38	4.38		1.86	.42	17.70	17.23	3.9
539	.262	3.32	7.32	10.38	15.05	9.86	14.29				2.11	2.11	60	1.76	.40	5.84	5.42	4.4
540	.263	3.33	7.35	10.37	15.05	9.86	14.30				2.10	2.10	40	1.77	.40	4.83	6.58	4.4
541	.265	3.32	7.33	10.28	14.91	9.76	14.16			1.33	4.45	5.78	60	1.61	.35	29.0	26.5	3.5
542	.265	3.32	7.33	10.08	14.91	9.76	14.16			1.34	4.44	5.78	30	1.60	.34	28.8	25.9	3.5
543	.266	3.33	7.35	10.26	14.89	9.74	14.13			2.06	4.49	6.55	30	1.62	.34	32.3	29.6	3.4
544	.265	3.32	7.32	10.26	14.88	9.74	14.13			2.07	4.50	6.58	30	1.65	.34	32.5	29.2	3.4
545	.264	3.30	7.28	10.25	14.86	9.74	14.12			2.43	4.50	6.95	60	1.64	.33	35.5	32.2	3.2
546	.266	3.32	7.32	10.24	14.86	9.73	14.12			2.83	4.50	7.33	60	1.66	.33	35.3	32.9	3.2
547	.264	3.30	7.27	10.23	14.84	9.73	14.11	279		3.44	4.58	8.02	50	1.58	.32	36.8	34.3	3.1
548	.263	3.29	7.25	10.23	14.84	9.72	14.10	278		3.42	4.60	8.01	60	1.58	.32	37.0	32.8	3.2
549	.265	3.31	7.30	10.24	14.85	9.74	14.12	279	42	3.42	4.57	7.82	60	1.58	.32	36.0	34.1	3.2
550	.263	3.29	7.26	10.24	14.85	9.73	14.11		41	2.81	4.58	7.39	30	1.57	.32	36.7	33.7	3.1
551	.267	3.34	7.35	10.25	14.87		14.12		42	2.95	4.52	7.46	60	1.60	.33	35.4	32.7	3.3
552	.267	3.33	7.35	10.25	14.86		14.11			2.94	4.50	7.45	60	1.60	.33	35.6	32.8	3.26
553	.266	3.32	7.32	10.24	14.85		14.11			4.09	4.57	8.67	50	1.58	.32	37.7	34.9	3.14
554	.266	3.32	7.32	10.24	14.85		14.11			4.00	4.58	8.57	60	1.57	.31	37.8	35.1	3.13
555	.179	2.28	5.03	10.16	14.74	9.92	14.39	276	37	0	0	0	60	2.12	.44	-10.7	-10.9	2.45
556	.180	2.29	5.05	10.16	14.74	9.92	14.39	276	37	0	0	0	60	2.04	.43	-11.4	-9.90	2.45
557	.179	2.26	4.98	10.06	14.59	9.83	14.25	277	38	2.13	5.90	8.04	40	1.86	.31	37.9	32.8	1.49
558	.179	2.26	4.98	10.06	14.59	9.82	14.24		39	2.14	5.92	8.06		1.83	.31	37.4	31.3	1.53
559	.183	2.30	5.06	10.05	14.58	9.81	14.23			3.18	6.50	9.76		1.66	.30	43.9	38.7	1.70
560	.183	2.30	5.08	10.05	14.58	9.81	14.23			2.84	6.60	9.45		1.63	.31	42.5	39.6	1.40
561	.181	2.27	5.00	10.04	14.56	9.80	14.22			4.72	6.76	11.48	60	1.51	.30	48.9	44.0	1.27
562	.182	2.29	5.04	10.04	14.56	9.80	14.22			4.69	6.60	11.29	50	1.51	.29	46.8	42.7	1.31
563	.182	2.29	5.05	10.06	14.59	9.82	14.25			0	6.67	6.67	50	1.61	.34	37.0	35.1	1.49
564	.181	2.29	5.04	10.09	14.63	9.84	14.27			0	6.54	6.54	40	1.90	.42	26.3	24.1	1.72
565	.183	2.30	5.06	10.06	14.59	9.82	14.24			2.75	6.59	9.34	50	1.55	.30	43.3	38.8	1.41
566	.183	2.30	5.08	10.10	14.64	9.85	14.29			0	5.64	5.64	30	1.87	.44	22.2	22.8	1.78
567	.182	2.30	5.06	10.10	14.65	9.86	14.30				4.89	4.89	40	1.75	.41	19.0	19.51	1.84
568	.182	2.30	5.07	10.12	14.68	9.87	14.32				3.16	3.16	40	1.91	.44	11.2	12.2	2.01
569	.182	2.30	5.08	10.13	14.69	9.89	14.34				1.89	1.89	40	1.98	.43	5.29	7.33	2.12
570	.181	2.29	5.05	10.12	14.67	9.87	14.32			3.25	0	3.25	60	1.80	.38	12.4	11.2	2.01

TABLE II. - Continued. DIFFUSER PERFORMANCE DATA

Reading	Diffuser inlet Mach number	Airflow rate		Inlet pressure				Inlet total temperature		Suction rate, percent			Exit profile (peak)			Diffuser, effectiveness, percent	Diffuser efficiency, percent	Total pressure loss, $\Delta P/P$, percent
		kg/sec	lb/sec	Total		Static		K	°F	Inner wall	Outer wall	Total	Position, percent of annular span	Value, v_{m2}/V_2	Value, v_{m2}/V_1			
				N/cm^2	psia	N/cm^2	psia											
Perforated plate A at 5 cm (2 in.); L/H = 2.0																		
571	0.259	3.33	7.34	10.45	15.16	9.94	14.42	276	36	0	0	0	60	1.93	0.41	-0.87	0.45	4.55
572	.260	3.33	7.35	10.45	15.15	9.94	14.42	276	36					1.95	.40	-1.19	.83	4.54
573	.261	3.34	7.37	10.45	15.16	9.95	14.42	276	37					2.01	.48	-1.14	3.47	4.5
574	.260	3.33	7.35	10.45	15.16	9.94	14.42							1.96	.47	-.99	2.91	4.4
575	.261	3.31	7.31	10.35	15.02	9.85	14.21			3.60		3.60	40	1.85	.45	20.7	22.5	3.6
576	.260	3.31	7.30	10.35	15.02	9.85	14.29			3.93		3.93		1.87	.45	21.3	22.3	3.6
577	.261	3.32	7.32	10.39	15.07	9.88	14.33			1.99		1.99		1.94	.47	14.3	15.6	3.9
578	.260	3.31	7.31	10.39	15.07	9.88	14.33			1.97		1.97		1.96	.47	14.3	15.1	3.9
579	.260	3.30	7.28	10.34	15.00	9.84	14.27			0	4.35	4.35		1.73	.39	23.9	22.6	3.6
580	.261	3.31	7.30	10.34	15.00	9.84	14.27			0	4.43	4.43		1.74	.38	24.0	22.7	3.8
581	.262	3.31	7.30	10.32	14.97	9.82	14.25			2.83	4.53	7.36		1.55	.33	29.4	27.8	3.4
582	.262	3.32	7.32	10.32	14.97	9.82	14.25			2.82	4.61	7.43		1.51	.33	29.2	28.2	3.4
583	.262	3.31	7.31	10.33	14.99	9.83	14.26			1.99	3.84	5.83		1.53	.33	25.9	24.3	3.5
584	.262	3.32	7.32	10.34	14.99	9.83	14.26			1.98	3.90	5.88	60	1.56	.32	25.2	23.2	3.6
585	.261	3.31	7.31	10.34	15.00	9.84	14.27			1.35	3.05	4.40	40	1.68	.38	24.1	23.7	3.6
586	.261	3.32	7.31	10.34	15.00	9.84	14.27			1.36	3.05	4.40		1.68	.38	23.6	22.4	3.6
587	.261	3.32	7.32	10.36	15.02	9.85	14.28			.94	2.47	3.41		1.78	.40	22.1	22.1	3.7
588	.259	3.30	7.27	10.36	15.03	9.86	14.30			.95	1.93	2.88		1.82	.42	20.0	20.0	3.7
607	.185	2.33	5.13	10.13	14.69	9.87	14.32	280	43	0	0	0	50	2.02	.41	-.92	-1.86	2.4
612	.184	2.31	5.10	10.10	14.64	9.85	14.28	278	41	2.48	0	2.48	50	1.97	.39	18.4	15.6	2.0
613	.183	2.31	5.09	10.08	14.63	9.83	14.26	278	41	4.63	0	4.63	50	1.80	.38	23.5	21.1	1.8
Perforated plate A at 1.3 cm (0.5 in.); L/H = 0.5																		
591	0.254	3.33	7.35	10.66	15.46	10.14	14.71	277	38	0	0	0	40	2.36	0.67	-49.5	-43.7	6.3
592	.255	3.34	7.37	10.66	15.46	10.14	14.71			0		0	40	2.36	.67	-49.5	-42.5	6.3
593	.257	3.32	7.33	10.54	15.28	10.02	14.53			3.88		3.88	60	2.02	.50	-20.5	-18.9	5.3
594	.258	3.34	7.36	10.54	15.28	10.02	14.54			3.85		3.85	60	1.98	.50	-21.1	-17.5	5.3
595	.259	3.34	7.37	10.53	15.28	10.02	14.53			0	4.20	4.20	40	2.27	.61	-20.4	-14.5	5.2
596	.258	3.34	7.36	10.54	15.28	10.01	14.52			0	4.14	4.14		2.25	.61	-20.2	-15.5	5.2
597	.261	3.34	7.36	10.44	15.14	9.92	14.39			2.31	4.12	6.43		2.04	.50	1.90	3.46	4.5
598	.184	2.33	5.13	10.14	14.70	9.89	14.34			3.99	6.33	10.32		1.84	.39	22.3	21.0	1.8
599	.183	2.32	5.12	10.13	14.70	9.89	14.34			3.96	6.37	10.33		1.72	.36	20.8	20.8	1.8
600	.260	3.33	7.34	10.44	15.14	9.92	14.38			2.69	4.14	6.83		2.03	.50	1.90	1.35	4.5
601	.259	3.33	7.34	10.48	15.20	9.96	14.44			1.93	3.50	5.43		2.14	.55	-8.56	-6.36	4.8
602	.260	3.34	7.34	10.48	15.20	9.95	14.43			1.94	3.53	5.47		2.15	.55	-7.13	-5.65	4.8
603	.182	2.31	5.09	10.16	14.74	9.91	14.38			2.85	5.30	8.16		2.08	.48	7.89	7.49	2.1
604	.182	2.31	5.09	10.16	14.73	9.91	14.38			2.85	5.37	8.22		2.06	.48	7.97	9.10	2.1
605	.183	2.32	5.12	10.15	14.73	9.91	14.37			3.30	5.35	8.65		1.99	.44	11.8	13.4	2.0
606	.182	2.31	5.09	10.16	14.73	9.91	14.37			3.34	5.45	8.79		1.99	.44	12.2	10.9	2.0

TABLE II. - Continued. DIFFUSER PERFORMANCE DATA

Reading	Diffuser inlet Mach number	Airflow rate		Inlet pressure				Inlet total temperature		Suction rate, percent			Exit profile (peak)			Diffuser effectiveness, percent	Diffuser efficiency, percent	Total pressure loss, $\Delta P/P$, percent
		kg/sec	lb/sec	Total		Static		K	°F	Inner wall	Outer wall	Total	Position, percent of annular span	Value, v_{m2}/V_2	Value, v_{m2}/V_1			
				N/cm^2	psia	N/cm^2	psia											
Perforated plate B at 2.5 cm (1 in.); L/H = 1.0																		
614	0.265	3.33	7.35	10.31	14.95	9.78	14.18	279	41	0	0	0	50	2.62	0.65	5.92	9.44	4.3
615	.266	3.34	7.37	10.31	14.95	9.78	14.18	279	↓	0	↓	0	↓	2.58	.64	5.35	9.68	4.3
616	.267	3.33	7.35	10.22	14.82	9.69	14.06	278	↓	4.19	↓	4.19	↓	2.46	.56	25.8	26.9	3.6
617	.266	3.32	7.33	10.23	14.84	9.70	14.07	↓	↓	3.01	↓	3.01	↓	2.49	.59	22.2	22.5	3.7
618	.267	3.33	7.35	10.23	14.84	9.70	14.07	↓	40	2.99	↓	2.99	↓	2.47	.59	21.3	23.0	3.7
619	.269	3.35	7.38	10.20	14.79	9.66	14.02	↓	↓	0	4.31	4.31	↓	2.34	.56	31.0	31.6	3.4
620	.268	3.34	7.35	10.19	14.78	9.66	14.02	↓	↓	0	4.33	4.33	↓	2.36	.57	30.3	31.0	3.4
621	.267	3.34	7.37	10.24	14.86	9.71	14.09	↓	↓	0	1.88	1.88	↓	2.46	.60	19.7	21.6	3.8
622	.264	3.30	7.28	10.25	14.86	9.73	14.11	↓	↓	1.68	0	1.68	↓	2.45	.61	16.6	19.3	3.8
623	.263	3.27	7.21	10.18	14.76	9.67	14.03	↓	↓	1.72	2.21	3.93	↓	2.36	.56	30.9	31.8	3.2
624	.267	3.33	7.34	10.19	14.78	9.67	14.02	↓	↓	1.68	2.15	3.83	↓	2.40	.56	30.9	31.6	3.3
625	.267	3.31	7.30	10.17	14.76	9.66	14.00	↓	↓	2.19	2.64	4.82	↓	2.30	.54	34.6	34.8	3.2
626	.268	3.32	7.33	10.18	14.76	9.65	14.00	↓	↓	2.17	2.63	4.81	↓	2.34	.54	34.3	34.7	3.2
627	.185	2.30	5.07	10.96	14.44	9.71	14.09	↓	41	3.18	3.86	7.03	↓	2.20	.50	42.4	42.2	1.4
628	.267	3.30	7.28	10.12	14.68	9.60	13.93	↓	↓	2.82	4.30	7.12	↓	2.25	.50	42.2	40.7	2.9
629	.186	2.30	5.07	9.93	14.40	9.68	14.04	↓	↓	4.12	6.41	10.53	40	2.07	.43	50.3	47.3	1.3
630	.186	2.30	5.07	9.92	14.39	9.67	14.03	↓	↓	6.47	6.77	13.24	40	2.03	.43	52.6	49.1	1.2
631	.267	3.29	7.25	10.12	14.66	9.59	13.92	↓	↓	4.40	4.56	8.96	50	2.17	.49	44.4	43.1	2.8
632	.266	3.29	7.25	10.10	14.65	9.56	13.90	↓	↓	4.39	4.55	8.94	↓	2.21	.49	45.3	43.0	2.8
633	.267	3.30	7.28	10.14	14.70	9.62	13.95	↓	↓	2.54	3.22	5.76	↓	2.30	.53	37.9	32.0	3.1
634	.267	3.30	7.27	10.13	14.69	9.61	13.93	↓	↓	2.55	3.45	6.00	↓	2.27	.52	38.5	36.9	3.06
635	.186	2.30	5.07	9.95	14.42	9.70	14.06	↓	↓	0	6.42	6.42	↓	2.39	.54	37.5	36.7	1.51
636	.185	2.29	5.06	9.94	14.4	9.70	14.06	↓	↓	0	6.44	6.44	↓	2.36	.55	37.3	36.7	1.50

TABLE II. - Continued. DIFFUSER PERFORMANCE DATA

Reading	Diffuser inlet Mach number	Airflow rate		Inlet pressure				Inlet total temperature		Suction rate, percent			Exit profile (peak)			Diffuser effectiveness, percent	Diffuser efficiency, percent	Total pressure loss, $\Delta P/P$, percent
		kg/sec	lb/sec	Total		Static		K	°F	Inner wall	Outer wall	Total	Position, percent of annular span	Value, v_{m2}/V_2	Value, v_{m2}/V_1			
				N/cm^2	psia	N/cm^2	psia											
Perforated plate B at 5 cm (2 in.); L/H = 2.0																		
637	0.267	3.38	7.44	10.38	15.06	9.84	14.28	279	42	0	0	0	50	2.49	0.59	12.4	14.3	4.1
638	.266	3.37	7.42	10.38	15.06	9.84	14.28	↓	41	0	↓	0	↓	2.48	.59	12.4	13.6	4.2
639	.266	3.35	7.39	10.33	14.98	9.80	14.21	↓	42	2.00	↓	2.00	↓	2.39	.53	23.7	24.0	3.7
640	.267	3.36	7.40	10.33	14.98	9.80	14.21	↓	42	2.02	↓	2.02	↓	2.37	.54	23.8	24.1	3.7
641	.267	3.35	7.39	10.30	14.94	9.77	14.18	278	41	3.54	↓	3.54	40	2.26	.52	30.1	30.0	3.4
642	.266	3.35	7.38	10.30	14.94	9.77	14.18	↓	↓	4.15	↓	4.15	40	2.23	.52	30.1	30.2	3.8
643	.266	3.34	7.36	10.29	14.93	9.77	14.17	↓	↓	0	2.89	2.89	50	2.31	.55	29.9	30.5	3.3
644	.267	3.35	7.38	10.27	14.90	9.75	14.14	↓	↓	0	4.24	4.24	↓	2.18	.52	34.5	34.3	3.2
645	.268	3.37	7.42	10.29	14.93	9.76	14.16	↓	↓	1.02	1.84	2.86	↓	2.23	.53	29.9	30.4	3.4
646	.266	3.34	7.37	10.29	14.92	9.76	14.16	↓	↓	1.02	1.88	2.90	↓	2.23	.53	30.2	30.5	3.4
647	.266	3.33	7.35	10.27	14.89	9.74	14.13	↓	↓	2.20	2.80	5.00	40	2.20	.50	34.2	32.8	3.2
648	.267	3.34	7.37	10.27	14.89	9.74	14.13	↓	↓	2.20	2.72	4.92	↓	2.14	.50	34.4	33.5	3.2
649	.181	2.27	5.00	10.05	14.58	9.82	14.24	↓	↓	3.27	4.17	7.44	↓	2.07	.46	38.0	37.8	1.4
650	.180	2.26	4.98	↓	14.58	9.82	14.84	↓	↓	3.29	4.15	7.44	↓	2.11	.47	38.1	37.4	1.4
651	.181	2.26	4.99	↓	14.57	9.81	14.23	↓	↓	3.18	4.58	8.03	↓	1.77	.41	41.6	40.9	1.3
652	.180	2.26	4.98	↓	14.57	9.81	14.23	279	↓	3.19	4.82	8.01	↓	1.81	.41	41.0	34.8	1.4
653	.267	3.33	7.34	10.25	14.86	9.72	14.09	↓	42	3.53	4.60	8.13	↓	1.99	.45	38.7	36.0	3.1
654	.267	3.33	7.34	↓	14.86	9.72	14.10	↓	42	3.54	4.52	8.06	↓	1.96	.46	39.1	37.8	3.0
655	.266	3.32	7.33	↓	14.87	9.73	14.12	↓	43	4.38	4.66	9.04	↓	2.06	.47	38.0	36.0	3.1
656	.267	3.33	7.34	↓	14.87	9.72	14.10	280	43	4.36	4.68	9.04	↓	2.01	.47	38.7	36.6	3.1
657	.166	2.08	4.58	10.02	14.53	9.82	14.25	281	45	5.50	7.50	13.0	50	1.62	.34	50.3	47.3	1.0
658	.182	2.27	5.00	10.04	14.57	9.81	14.73	281	45	5.08	6.86	11.94	50	1.60	.35	47.4	45.7	1.2
659	.181	2.25	4.96	10.05	14.57	9.81	14.22	282	47	4.41	5.68	10.09	40	1.97	.45	44.4	42.2	1.3
660	.181	2.26	4.97	10.05	14.57	9.81	14.23	281	46	4.35	5.63	9.99	40	1.87	.40	44.2	42.7	1.3

TABLE II. - Concluded. DIFFUSER PERFORMANCE DATA

Reading	Diffuser inlet Mach number	Airflow rate		Inlet pressure				Inlet total temperature		Suction rate, percent			Exit profile (peak)			Diffuser effectiveness, percent	Diffuser efficiency, percent	Total pressure loss, $\Delta P/P$, percent
		kg/sec	lb/sec	Total		Static		K	°F	Inner wall	Outer wall	Total	Position, percent of annular span	Value, v_{m2}/V_2	Value, v_{m2}/V_1			
				N/cm^2	psia	N/cm^2	psia											
Perforated plate B at 1.3 cm (0.5 in.); L/H = 0.5																		
661	0.263	3.36	7.40	10.47	15.19	9.94	14.41	279	42	0	0	0	50	2.77	0.71	-16.8	-9.60	5.1
662	↓	3.36	7.40	10.47	15.18	9.94	14.42	↓	↓	0	↓	0	↓	2.76	.71	-17.1	-9.16	5.1
663		3.35	7.38	10.42	15.11	9.90	14.36			2.12		2.12		2.67	.66	-4.02	2.03	4.6
664		3.35	7.38	10.42	15.12	9.90	14.35			2.11		2.11		2.67	.66	-3.96	2.46	4.6
665		3.33	7.34	10.36	15.03	9.84	14.27			3.83		3.83		2.66	.63	8.35	11.43	4.2
666		3.32	7.33	10.36	15.03	9.84	14.27			4.36	↓	4.36		2.65	.62	8.67	11.7	4.1
667	↓	3.33	7.33	10.37	15.04	9.86	14.30			0	2.89	2.89		2.59	.64	4.32	10.0	4.2
668	.264	3.34	7.36	10.37	15.05	9.86	14.29				2.92	2.92		2.64	.63	4.98	9.71	4.3
669	.262	3.31	7.30	10.34	15.00	9.83	14.26				4.11	4.11		2.50	.61	11.5	15.7	3.9
670	.263	3.31	7.30	10.34	15.00	9.82	14.24		↓		4.18	4.18		2.63	.61	12.0	14.7	4.0
671	.181	2.28	5.02	10.07	14.61	9.83	14.26		43	↓	6.42	6.42		2.44	.57	21.5	23.1	1.7
672	.181	2.27	5.00	10.08	14.62	9.84	14.27	↓	43	6.71	0	6.71		2.35	.60	17.6	20.8	1.8
673	.262	3.31	7.29	10.37	15.03	9.85	14.29	280	45	1.14	1.95	3.09		2.58	.63	6.64	11.25	4.1
674	.261	3.30	7.27	10.36	15.03	9.85	14.29	280		1.15	1.99	3.14		2.67	.63	6.93	10.85	4.1
675	.264	3.31	7.31	10.31	14.95	9.80	14.21	281		2.19	3.26	5.45		2.50	.58	19.9	23.3	3.7
676	.263	3.30	7.28	10.31	14.95	9.79	14.20	↓		2.25	3.24	5.49		2.45	.58	20.9	22.4	3.7
677	.178	2.23	4.91	10.06	14.60	9.83	14.25			3.26	4.99	8.25		2.42	.54	33.9	31.6	1.5
678	.178	2.23	4.92	10.06	14.59	9.82	14.24		↓	3.35	5.02	8.36		2.33	.53	33.7	32.6	1.5
679	.266	3.31	7.30	10.26	14.88	9.75	14.13		46	3.76	4.26	8.02		2.46	.53	34.1	34.5	3.2
680	.265	3.31	7.29	10.26	14.88	9.74	14.13			3.67	4.31	7.99		2.50	.53	34.6	34.4	3.2
681	.179	2.23	4.92	10.03	14.55	9.79	14.21			5.62	6.66	12.29		2.19	.46	51.2	47.8	1.2
682	.180	2.24	4.93	10.03	14.55	↓	14.21			5.67	6.71	12.38		2.26	.47	49.9	47.0	1.2
683	.180	2.24	4.93	10.03	14.54		14.19			6.83	6.71	13.54		2.19	.46	53.9	49.3	1.1
684	.181	2.25	4.97	10.02	14.54	↓	14.19	↓	↓	6.84	6.69	13.5		2.22	.46	53.5	49.5	1.1
685	.266	3.32	7.31	10.24	14.85	9.72	14.10	280	44	4.45	4.32	8.77		2.38	.52	37.7	37.2	3.0
686	.266	3.32	7.32	10.24	14.85	9.72	14.10			4.44	4.23	8.67		2.38	.52	37.3	36.9	3.1
687	.180	2.25	4.96	10.04	14.56	9.80	14.22			4.42	5.78	10.20		2.27	.49	44.2	42.2	1.3
688	.180	2.25	4.96	10.04	14.56	9.80	14.22	↓	↓	4.47	5.80	10.28	↓	2.28	.49	44.0	41.8	1.3

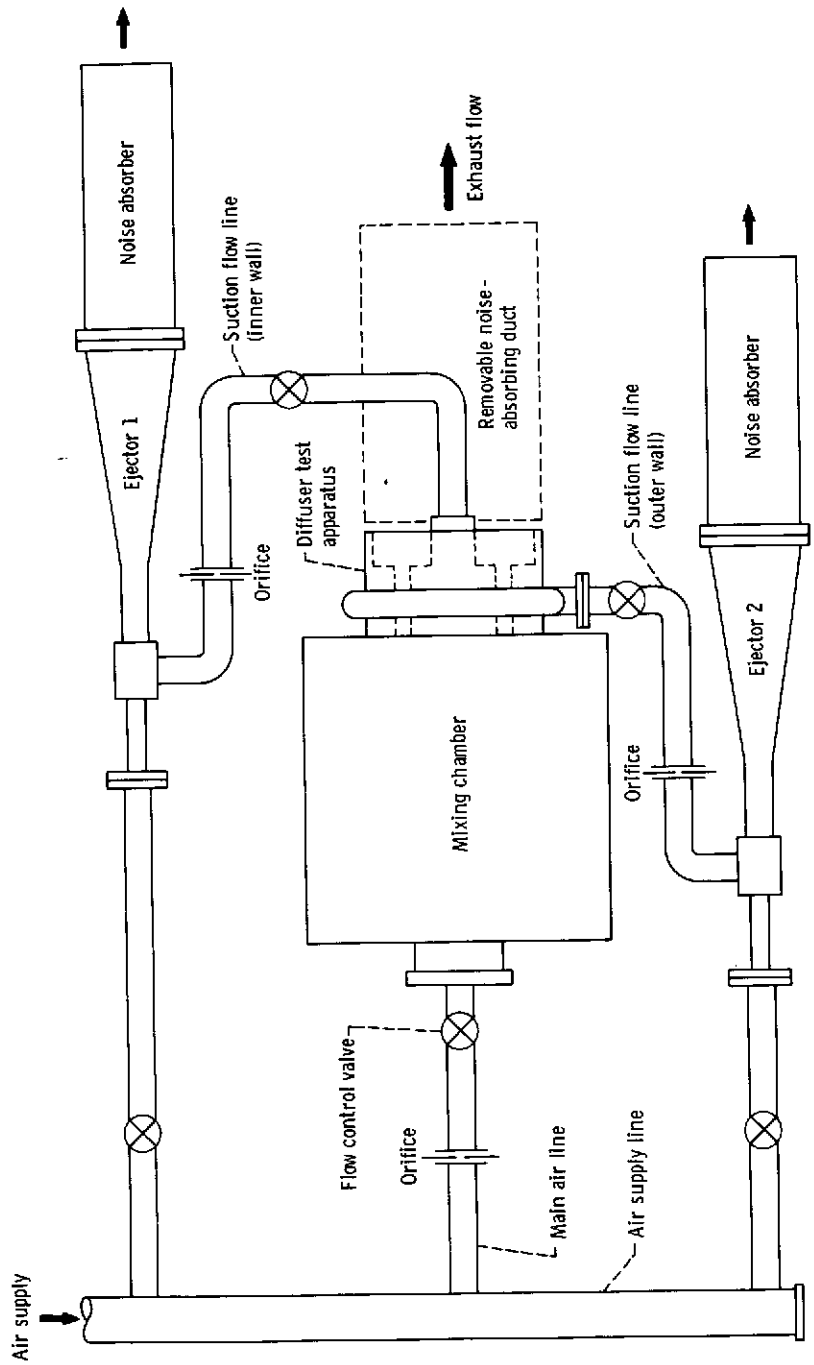

Figure 1. - Flow system.

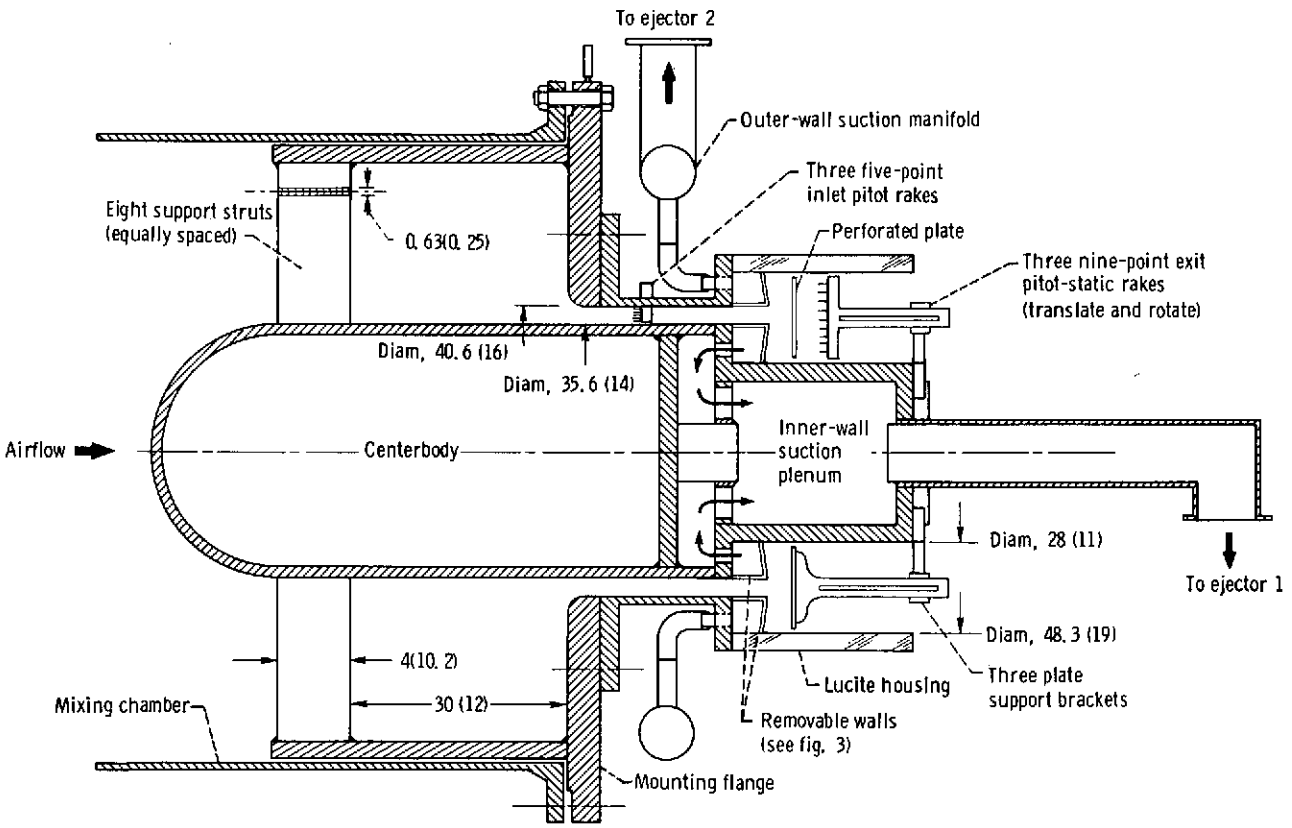

Figure 2. - Cross section of asymmetric annular diffuser test apparatus. (Dimensions are in cm (in.).)

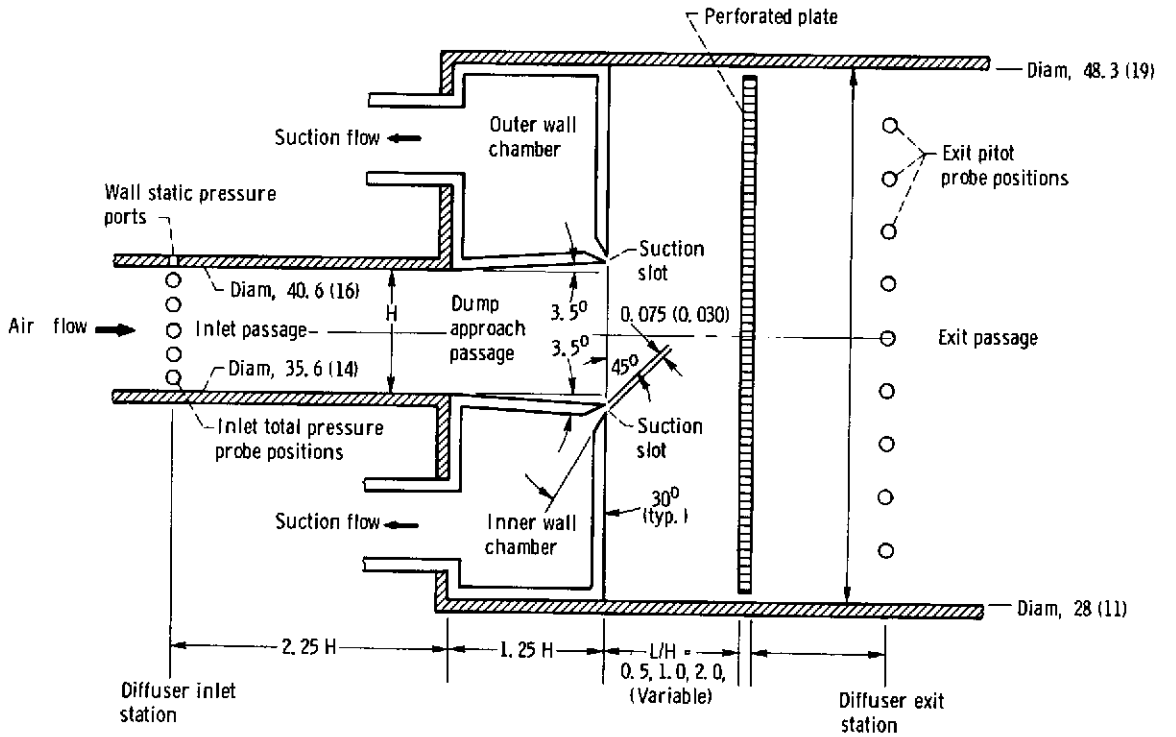

Figure 3. - Diffuser passage details. Inlet passage height, H, 2.54 centimeters (1.0 in.). (Dimensions are in cm (in.) unless otherwise indicated.)

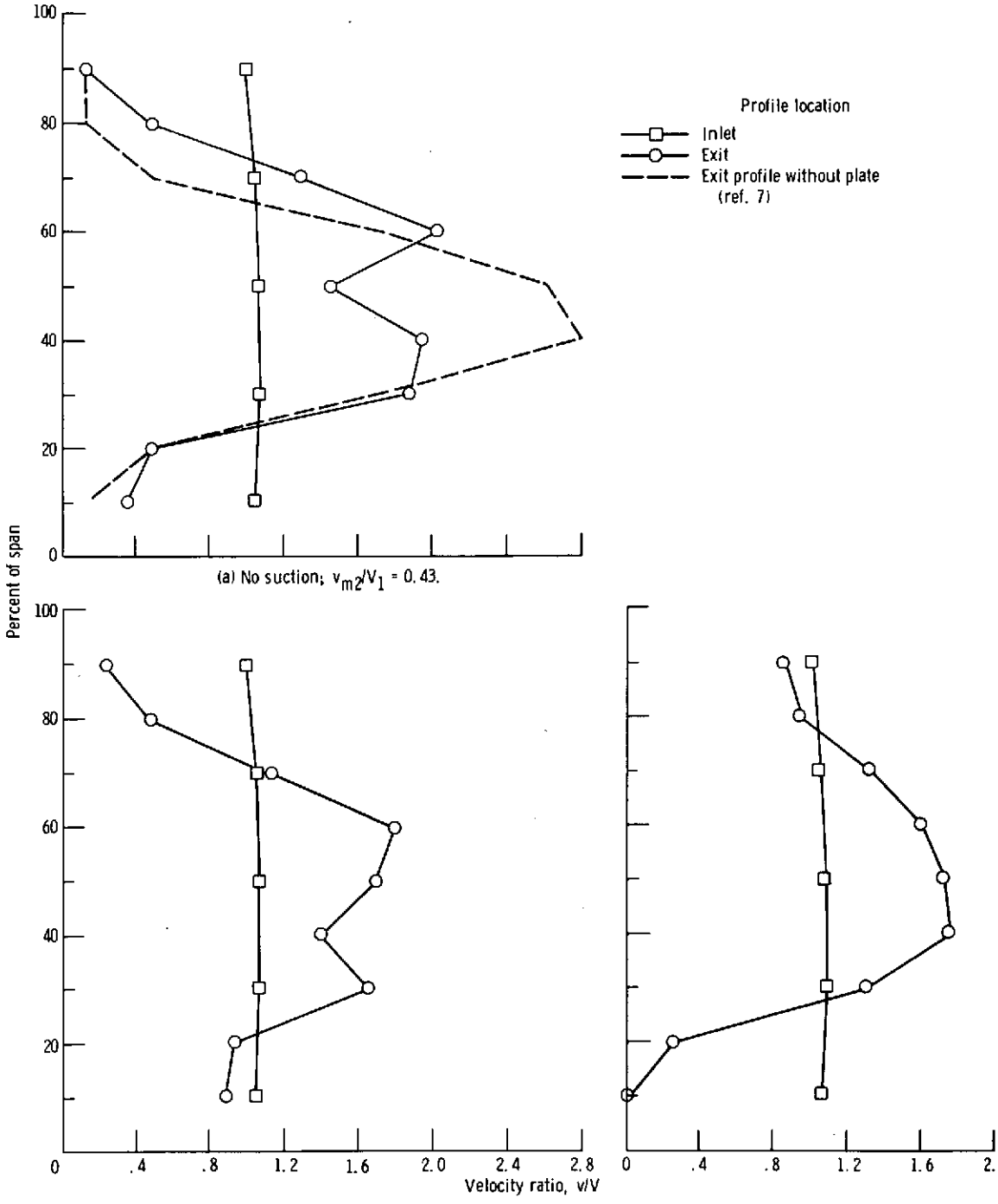

Figure 4. - Radial profiles of diffuser inlet and exit velocity at various suction rates with perforated plate A at L/H = 1.0. Inlet Mach number $M_1 = 0.180$.

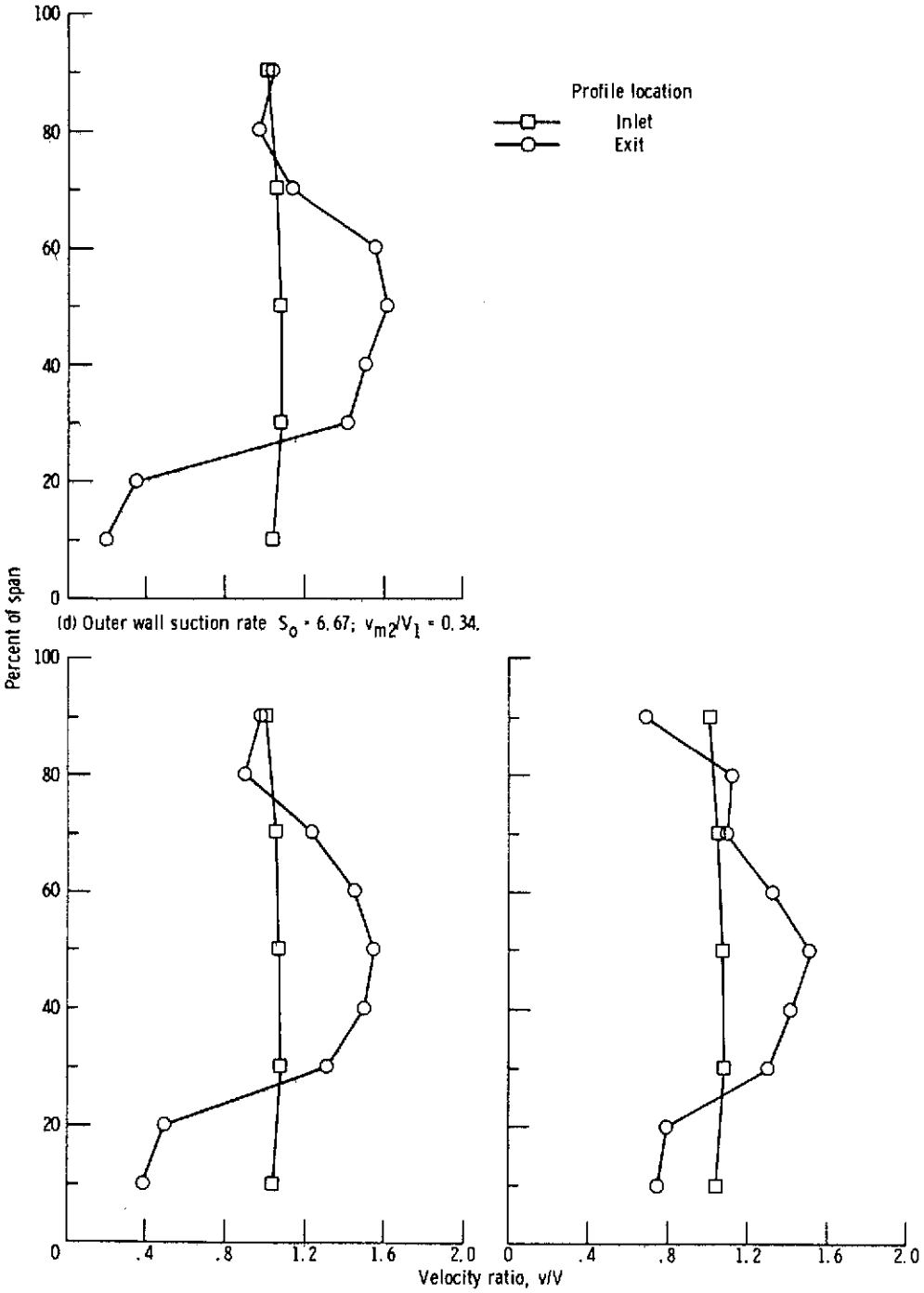

(d) Outer wall suction rate $S_o = 6.67$; $v_{m2}/V_1 = 0.34$.

(e) Inner wall suction rate $S_i = 2.75$; outer wall suction rate $S_o = 6.59$; total suction rate $S_t = 9.34$; $b_i = 0.295$; $b_o = 0.705$; $v_{m2}/V_1 = 0.30$.

(f) Inner wall suction rate $S_i = 4.69$; outer wall suction rate $S_o = 6.60$; total suction rate $S_t = 11.29$; $b_i = 0.42$; $b_o = 0.58$; $v_{m2}/V_1 = 0.29$.

Figure 4. - Concluded.

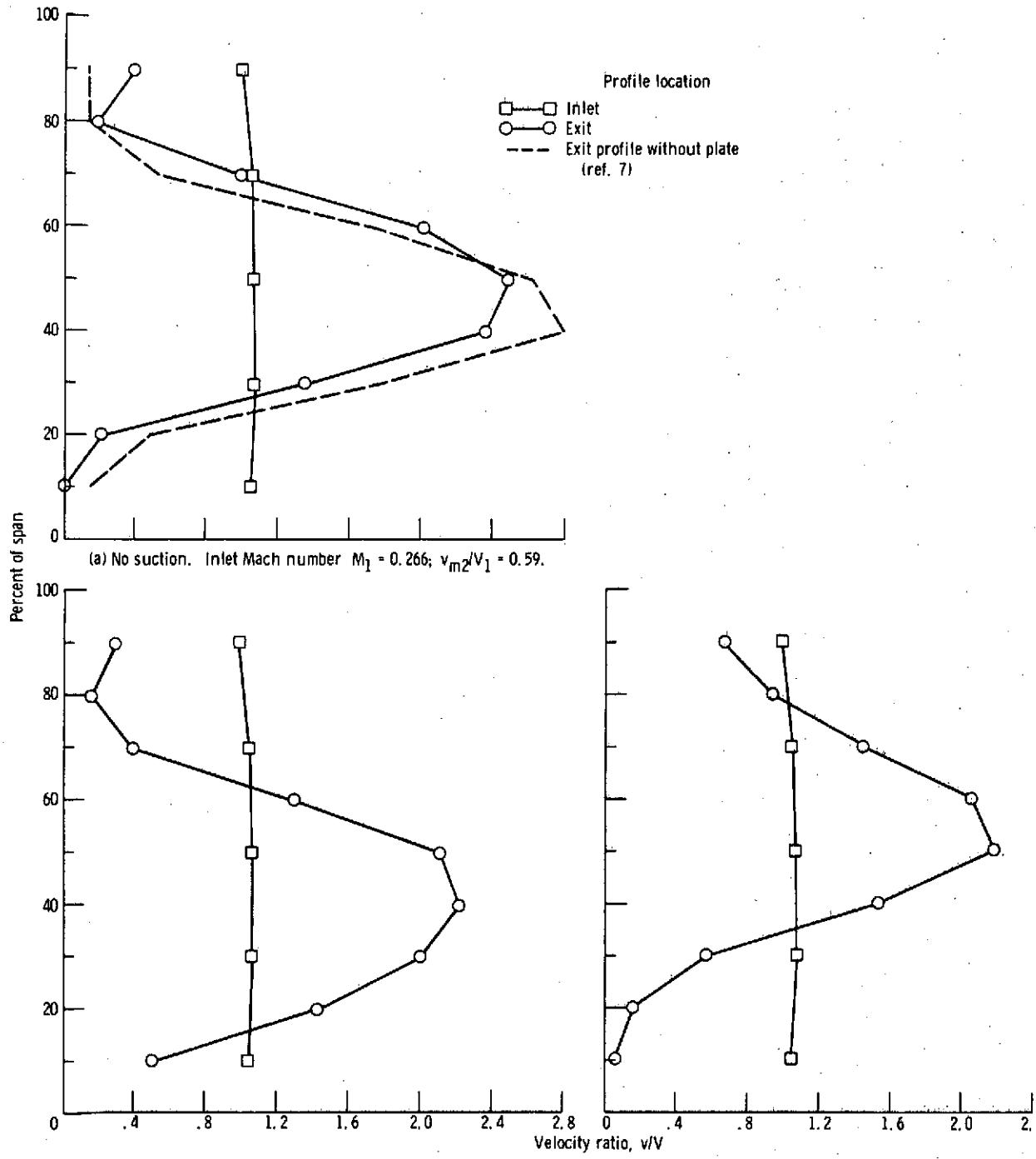

(a) No suction. Inlet Mach number $M_1 = 0.266$; $v_{m2}/V_1 = 0.59$.

(b) Inner wall suction rate $S_i = 4.15$; inlet Mach number $M_1 = 0.266$; $v_{m2}/V_1 = 0.52$.

(c) Outer wall suction rate $S_o = 4.24$; inlet Mach number $M_1 = 0.267$; $v_{m2}/V_1 = 0.52$.

Figure 5. - Radial profiles of diffuser inlet and exit velocity at various suction rates with perforated plate B at L/H = 2.0. Inlet Mach number M_1 as indicated.

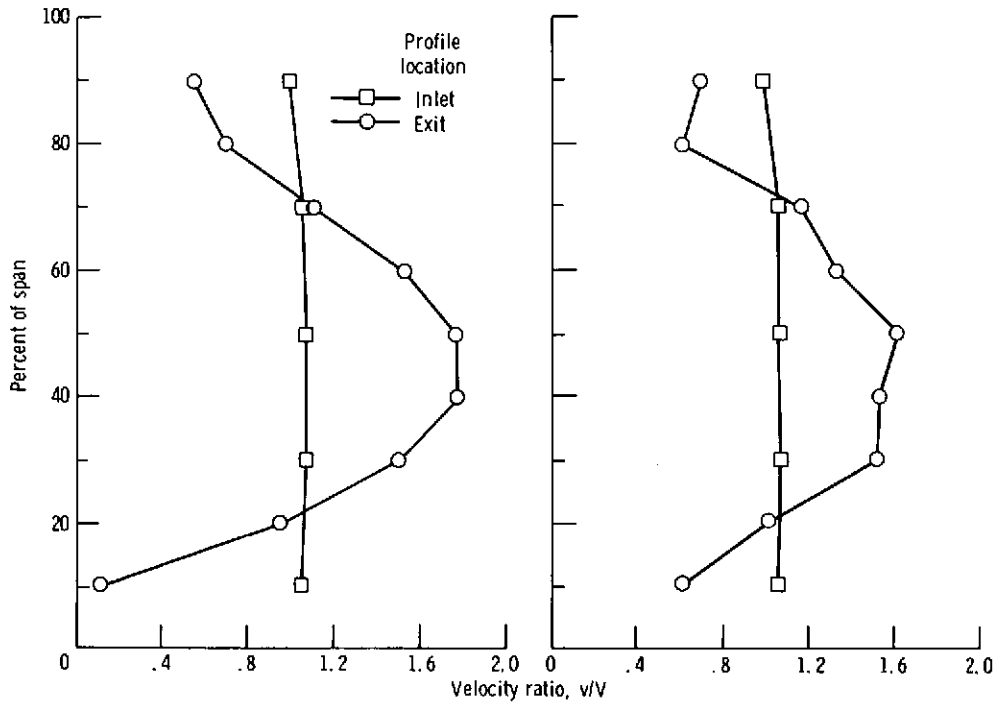

(d) Inner wall suction rate $S_i = 3.18$; outer wall suction rate $S_o = 4.85$; total suction rate $S_t = 8.03$; $b_i = 0.40$; $b_o = 0.40$; $b_o = 0.60$; inlet Mach number $M_1 = 0.181$; $v_{2m}/V_1 = 0.41$.

(e) Inner wall suction rate $S_i = 5.5$; outer wall suction rate $S_o = 7.5$; total suction rate $S_t = 13.0$; $b_i = 0.42$; $b_o = 0.58$; inlet Mach number $M_1 = 0.166$; $v_{2m}/V_1 = 0.34$.

Figure 5. - Concluded.

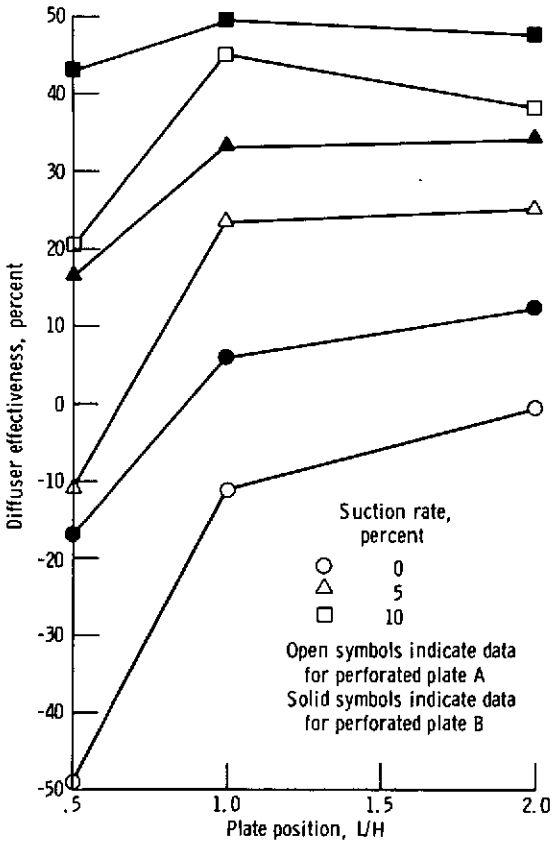

Figure 6. - Effect of perforated plate geometry and plate position on diffuser effectiveness.

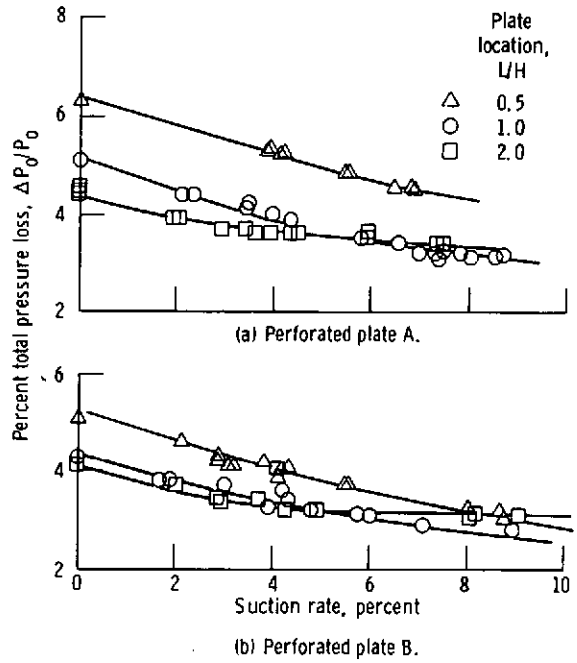

Figure 7. - Effect of suction on diffuser total pressure loss for perforated plates A and B at three locations. Inlet Mach number, M_1, 0.26.